Magazine of Civil Engineering. 2019. 92(8). Pp. 48–62
Инженерно-строительный журнал. 2019. № 8(92). С. 48–62

Magazine of Civil Engineering

ISSN 2071-0305

journal homepage: http://engstroy.spbstu.ru/

DOI: 10.18720/MCE.92.4

Bending and torsion behaviour of CFRP strengthened RC beams

R. Al-Rousan*, I. Abo-Msamh
Jordan University of Science and Technology, Irbid, Jordan,
** E–mail: rzalrousan@just.edu.jo*

Keywords: engineering, materials science, technology, civil engineering, structural concrete

Abstract. In the construction industry, there is growing attention of using effective external strengthening techniques such as bonding of Carbon Fiber Reinforced Polymers (CFRP) composites onto the external deficient faces of the structural members due to their ease of installation, low invasiveness, high corrosion resistance, and high strength to weight ratio. As a result, the center of consideration of the majority of previously published studies was either only on the impact of fibers on the structural behavior of reinforced concrete elements or using CFRP composite as external strengthening for flexural or shear. The intent was to arrive at the vital CFRP strengthening technique that provides an effective increase in the flexural and shear strength while maintaining ductile failure mode. Therefore, this paper investigated the behavior of simply supported RC beams strengthened using CFRP and subjected to combined bending and torsion using Nonlinear Finite Element Analysis (NLFEA). Twenty-six models have been constructed and divided into six groups to scrutinize the effect of clear span to depth ratio; CFRP length; CFRP strip spacing; and CFRP depth. The results showed that the increase in the clear span to depth ratio as well as length of CFRP leads to a notable increase in the ductility and decreases the ultimate load. The models with zero spacing CFRP strips (Fully) showed a higher considerable effect than the models with strips wrapping. Furthermore, this enhancement was the highest for group six which contains the models with the highest CFRP depth.

1. Introduction

Effect of combined bending and torsion occurs if the beam is loaded with out of plane eccentricity. Where the load is located away from the shear center axis which results in twisting the structural member with an undesirable brittle mode of failure. Although torsion is considered as a secondary effect compared to the flexural effect. Also, the torsion is negligible in most cases during the designing process. It is not the case for reinforced concrete (RC) structural members which are exposed to torsional loading in addition to the shear and flexure. The edge beams located on each floor of multi-story buildings, ring beams, spiral stairs, spandrel beams and flanged beams with T cross-section are exposed to torsion, shear, and flexure [1, 2].

Some experimental studies had been performed with different load setups to study the effect of pure shear. Pure bending combined bending and torsion or combined shear and torsion [3–5]. The effect of span length of cantilever RC beams under pure torsion had been studied using a non-linear finite element analysis. The results showed that when the span/depth ratio is equal to 4 or more, the beams have the same torsional strength but less than the beams that have smaller ratios [6]. The Modified Compression Field Theory (MCFT) was evaluated for reinforced and prestressed concrete beams subjected to combined bending and torsion. It was concluded that the MCFT could accurately determine the full behavior of such beams compared to the experimental results [7].

Existing structures may need torsional strengthening or rehabilitation due to several reasons. Some of these reasons are the increase in service load, inadequate design, change on the structure utilization, an improvement in the code regulations and seismic problems in some cases. Using Fiber Reinforced Polymers (FRP) as a strengthening material is the most recent and promising technology. It is a flexible material that can be made in any desired shape and can be introduced through a structural member either externally or internally. It is preferable in civil engineering applications because it is high corrosion resistance, high strength,

Al-Rousan, R., Abo-Msamh, I. Bending and torsion behaviour of CFRP strengthened RC beams. Magazine of Civil Engineering. 2019. 92(8). Pp. 48–62. DOI: 10.18720/MCE.92.4

Аль-Рушан Р., Або-Мсамх И. Поведение при изгибе и кручении железобетонных балок, усиленных композитным углеволокном // Инженерно-строительный журнал. 2019. № 8(92). С. 48–62. DOI: 10.18720/MCE.92.4

high stiffness, excellent fatigue performance, low weight, easy installation and good resistance to chemical attacks [8–11].

The efficiency of using CFRP for the torsional strengthening of RC beams had been studied either for rectangular or T-cross sections when subjected to pure torsion in most studies. Studying the combined effect of bending and torsion can be hardly found in the literature. Using the CFRP material can significantly increase the torsional strength and ductility. However, this enhancement can be affected by several factors such as concrete class, reinforcement ratio, number of layers, strip spacing, and wrapping scheme. Although the fully wrapping scheme is the best wrapping scheme, the difficulties of its application tend to use the U strip wrapping instead of fully wrapping. It is also recommended to increase the number of layers and decreasing the distance spaced between CFRP strips [12–18].

A new model was developed to predict the full behavior till failure of the strengthened RC beams subjected to torsion. Good agreements with the experimental results were achieved by that model comparing the torsional strength, FRP strain, and failure modes for different wrapping configurations [19]. To reduce the complexity of load setup, effort, time and cost during the experimental testing, ANSYS software had been used by many researchers. It was recommended about this software to be used since their results achieved good agreement with experimental results [20–24]. Therefore, essential issues to produce effective, economical, and successful CFRP strengthening were discussed. Also, the impact of CFRP external strengthening on the behavior of reinforced concrete beams subjected to bending and torsion received miniature consideration. The scientific problem considered in the study is indeed one of the problems in the modern theory of reinforced concrete. Despite a significant number of studies on the problem of bending with torsion, to date. There are no sufficiently reliable solutions to this problem that most fully reflect the physical nature of the problem. As a result, the torsional behavior of simply supported RC beams subjected to combined bending and torsion is studied using the nonlinear finite element analysis (NLFEA). For this purpose, validation against the previous experimental study reported by Gesund et al. [25] is firstly simulated. After that, a parametric study is extended for strengthened RC beams using different configurations of CFRP in terms of clear span to depth ratio, CFRP length, CFRP depth, and CFRP strips c-c spacing.

2. Methods

The NLFEA is a numerical method used to simplify the analysis of a variety of engineering problems. Also, to obtain their approximate solutions at a lesser cost, time, and effort compared to experimental testing. ANSYS is a general-purpose software used in this study. Twenty-six full-scale models strengthened using CFRP are developed to carry out different investigated parameters.

The experimental work performed by Gesund et al. [25] was used to validate the finite element model in this study. A total of twelve simply supported RC beams tested until failure under combined bending and torsion (Figure 1). The cross-section of the beam is 200 × 200 mm with a 1600 mm clear span length. All beams were reinforced using three bars of tension reinforcement and two bars of compression reinforcement with a 13 mm nominal diameter. Besides, a 10 mm nominal diameter for closed stirrups was applied at 50 mm spacing c-c (Figure 1). The beams were loaded by two-point loads at the end of two-moment arms providing out of plane eccentricity. Hence the beams were subjected to the combined effect of bending and torsion (Figure 1).

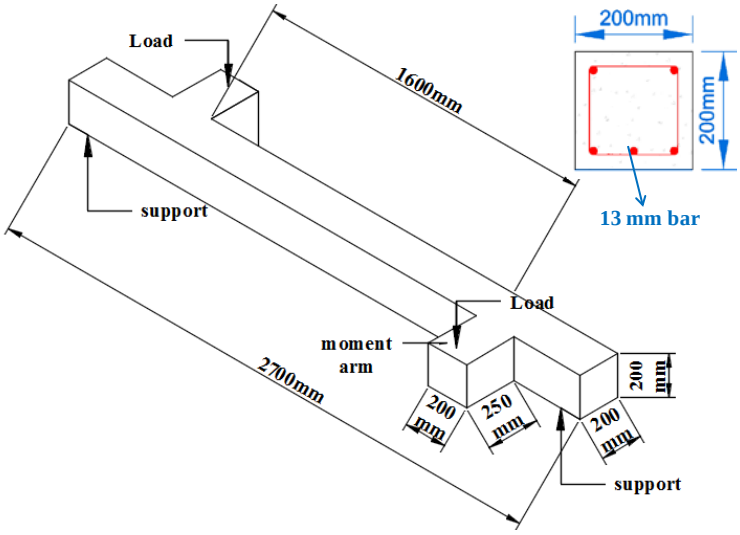

Figure 1. View of the model under load [25].

2.1. Experimental Work Review

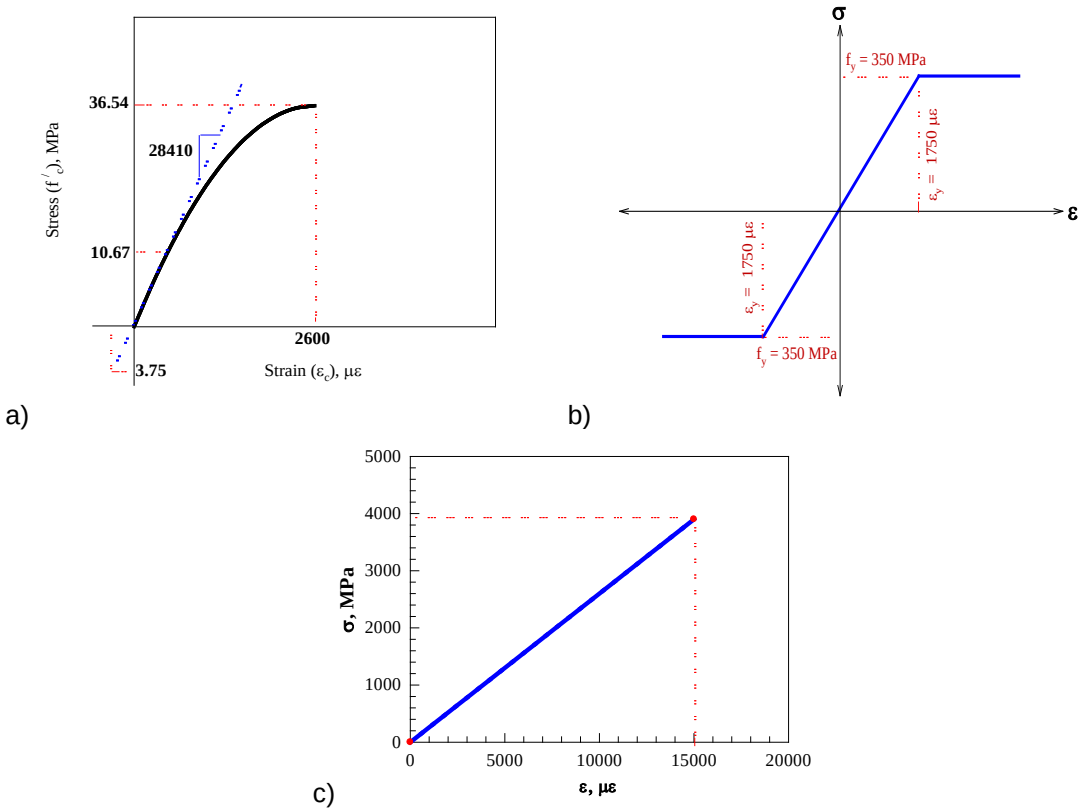

Figure 2. Stress-Strain Curve for (a) Concrete, (b) Steel, and (c) CFRP composite.

2.2. Description of Non-linear Finite Element Analysis (NLFEA)

SOLID 65 is used to model the concrete which is suitable for tension cracking, crushing in compression and plastic deformations. It is a three-dimensional element defined by eight nodes. Each node has three degrees of freedom with a presence of translations in the three nodal directions; x, y, and z for each node. Steel reinforcement is modeled using link 180, which is a uniaxial tension-compression element. It includes two nodes, and each node has three degrees of freedom. This element can predict large deflection, large strain, rotation, creep, and plasticity. SOLID 45 is used to model the loading and supporting steel plates. This element is suitable to model the dimensional solid structures defined by eight nodes. There is a presence of translations in the three nodal directions; x, y, and z for each node. This element can predict large deflection, large strain, stress stiffening, creep, and plasticity. For CFRP, the SHELL 181 element type, having four nodes is used in modeling. It is chosen because it is appropriate to analyze thin layered applications. Three translations and three rotations are considered to include the six degrees of freedom at each node.

Concrete is a brittle material having high compressive strength compared to tensile strength. The cylindrical compressive strength of concrete is 36.54 MPa. The elastic modulus of elasticity (Ec) and modulus of rupture (f_r) of concrete are 28410 MPa and 3.75 MPa, respectively, as shown in Figure 2(a). Concrete poison's ratio is assumed 0.17 for all models. Shear transfer coefficient for open and closed cracks, βt and βc respectively, are important inputs needed for concrete, which indicate the condition of crack surface. In this study, a value of 0.2 and 0.9 is set for the βt and βc, respectively. Steel reinforcement is modeled as a bilinear isotropic material with 200 GPa for the elastic modulus of elasticity and 0.3 of poison's ratio. Its behavior is assumed to be elastic-perfectly plastic, and the same assumption is set for tension and compression reinforcement with yielding stress of 350 MPa, as shown in Figure 2(b). Steel plates are added to the finite element model to avoid stress concentrations at the support and loading locations. These plates are steel type and defined as linear elastic isotropic material with 200 GPa for the elastic modulus of elasticity and 0.3 of poison's ratio. Sika Wrap Hex 300C 0/90 is the CFRP type used in this study. It is a bi-directional material property with 0.166 mm thickness and having fibers in longitudinal and transverse directions. The linear elastic tensile stress-strain curve for CFRP composites is shown in Figure 2(c) and the detailed mechanical properties and poison's ratio in all directions, are shown in Table 1.

Table 1. CFRP composites properties.

Modulus of elasticity (GPa)		Poison's ratio		Shear modulus of elasticity (GPa)		Ultimate tensile strength (MPa)	Ultimate strain
E_x	260	V_{xy}	0.22	G_{xy}	106.6		
E_y	260	V_{yz}	0.22	G_{yz}	106.6	3900	0.015
E_z	4.5	V_{zx}	0.30	G_{zx}	1.73		

The concrete beam and steel plates were modeled as solid elements while steel reinforcement was modeled as link elements. In the case of strengthened RC beams, the CFRP sheets were modeled as shell element with a mesh size of 25 mm. To ensure the perfect bond between concrete and reinforcement, the link element of steel is connected between each adjacent Solid 65 elements, hence the same nodes are shared between the two materials. The same approach is used for the CFRP sheets to provide the perfect bonding as well as for the Steel plates. The geometry of the control and strengthened model, along with the reinforcement specimens are shown in Figure 3(a), Figure 3(b) and Figure 3(c), respectively. The meshing of the CFRP sheet for both fully U wraps and strips wrapping is also shown in Figure 3(d) and Figure 3(e), respectively.

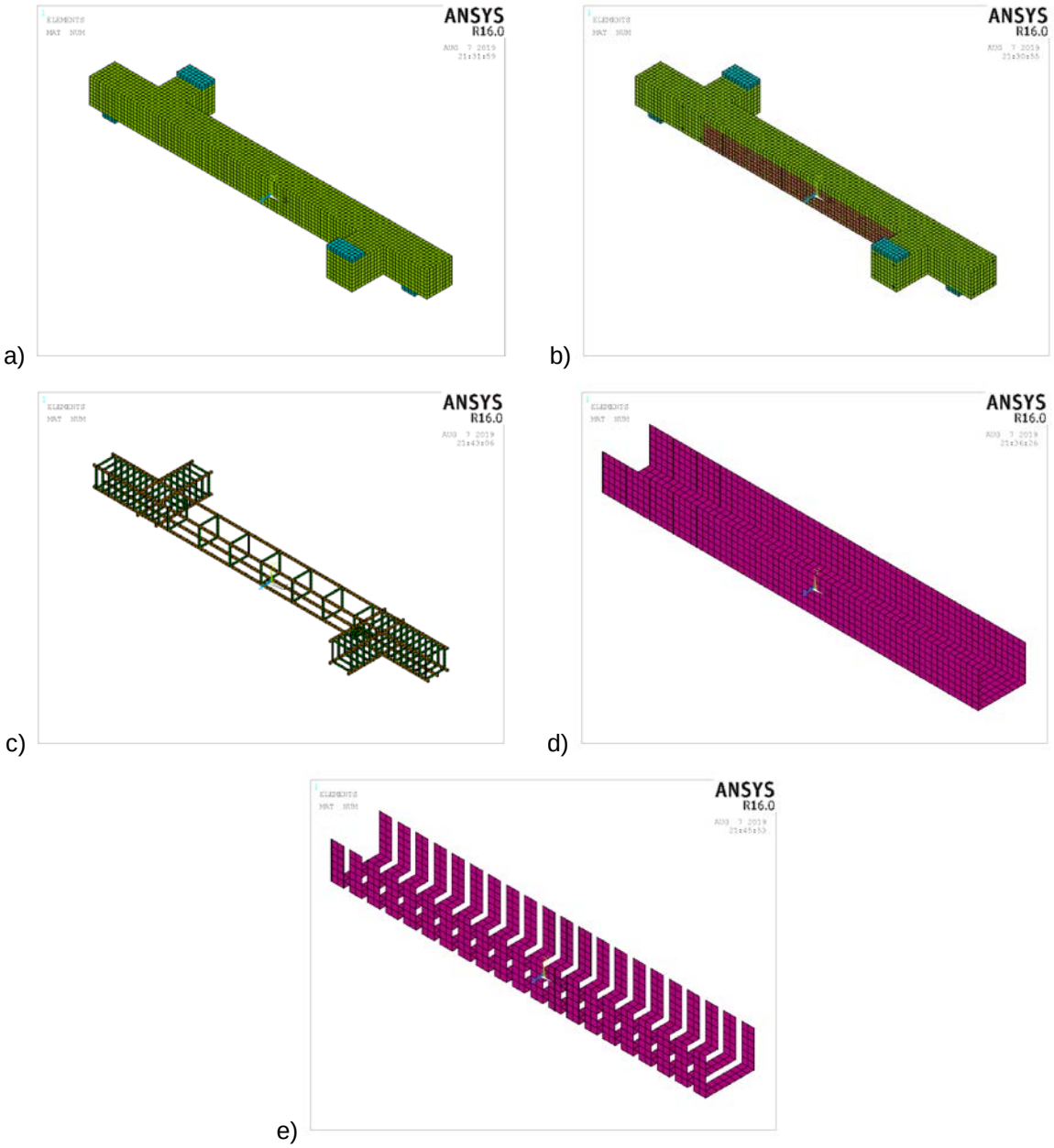

Figure 3. Geometry and meshing.

The loads are applied on the two steel plates at the end of the moment arms as line loads distributed over nine nodes. The purpose of these moment arms is to provide the twisting of the main beam. To constrain the model, displacement boundary conditions are required. At the left end of the beam the Ux, Uy, and Uz displacements are set to zero to ensure hinge support. While roller support is added at the right end of the beam by setting zero value to the Uy displacement. Figure 4 shows the loads and boundary conditions of the model. The total applied load is divided into multiple load steps or load increments. Newton–Raphson equilibrium iterations give convergence at the end of each load increment within tolerance limit equal to (0.001) and a load increment of 0.22 kN. When large numbers of cracks appear throughout the concrete, the loads are applied gradually with smaller load increments.

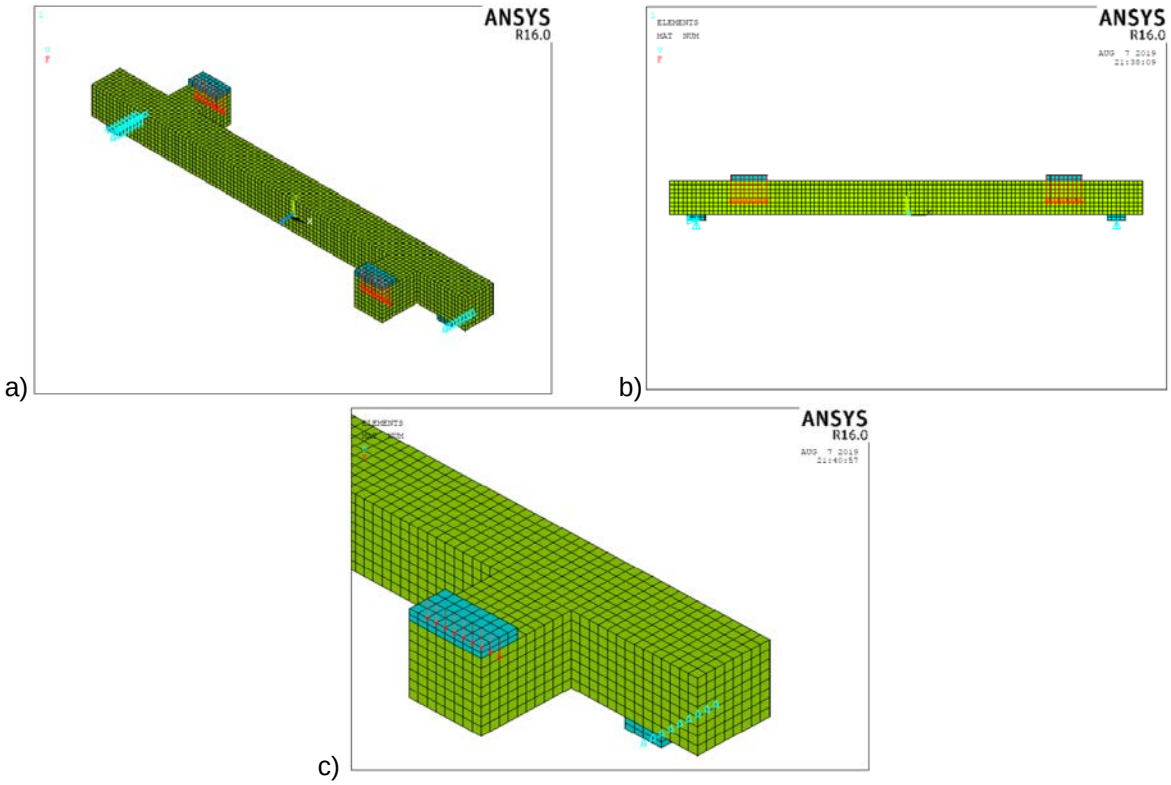

Figure 4. Loads and boundary conditions: (a) 3-D view, (b) Front view, and (c) Zoomed view.

2.3. Investigated Parameters

Twenty-six full-scale models strengthened using CFRP are developed to carry out different investigated parameters. A parametric study conducted in this research consists of six groups. The first group contains three models to study the effect of a clear span to depth ratio. 8, 6, and 4 are the clear span to depth ratios used. These models are strengthened using fully CFRP U wrap along the clear span length, and BC3 with ratios 8, 6, and 4 respectively. The other groups are modeled with the ratio equal to 8. Group 2 includes three models with different lengths of 1600 mm, 1100 mm and 800 mm. The rest four groups study the effect of two parameters; CFRP depth, and CFRP strip spacing. Four different CFRP depths of 50 mm, 100 mm, 150 mm, and 200 mm are studied for groups 3, 4, 5, and 6, respectively. Each depth group includes five models with different c-c spacing between 50 mm U strips, which are 225 mm, 175 mm, 125 mm, 75 mm and zero spacing. Figure 5 and Figure 6 show the schematic representation of CFRP strengthening configurations for the two cases of fully U-wrap and 50 mm U strip wrapping, respectively. A full description of the finite element modeling groups is shown in Table 2.

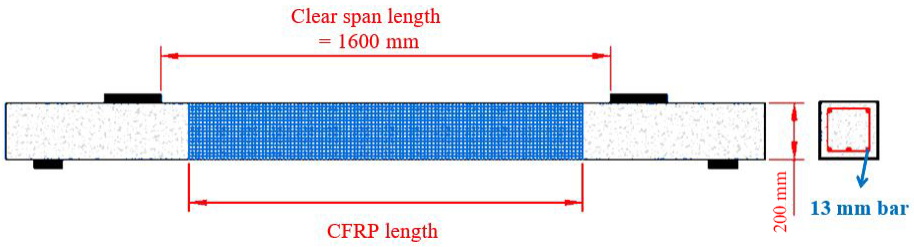

Figure 5. Schematic representation of fully CFRP U-WRAP.

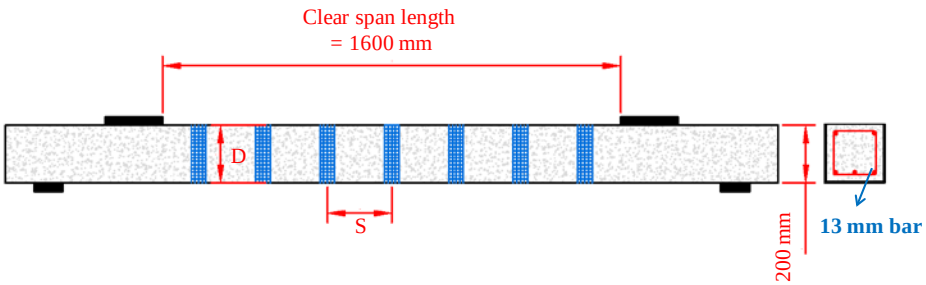

Figure 6. Schematic representation of 50 mm U strip wrapping where S is the c-c spacing between CFRP strips, and D is the CFRP depth.

Table 2. Investigated parameters.

Group number	Parameter	Beam number	Test section to depth ratio			CFRP strengthening configuration	CFRP length (mm)	CFRP Depth (mm)
			Clear span length (mm)	Depth (mm)	Ratio			
1	Clear span length to depth ratio	B1	1600	200	8	Fully FRP U wrap	1600	200
		B2	1200	200	6	Fully FRP U wrap	1200	
		B3	800	200	4	Fully FRP U wrap	800	
2	CFRP length	B4	1600	200	8	Fully FRP U wrap	1600	200
		B5	1600	200	8	Fully FRP U wrap	1100	
		B6	1600	200	8	Fully FRP U wrap	800	
3	CFRP depth	B7	1600	200	8	50 mm U strip wrapping at 225 mm c/c	1600	50
		B8	1600	200	8	50 mm U strip wrapping at 175 mm c/c		
		B9	1600	200	8	50 mm U strip wrapping at 125 mm c/c		
		B10	1600	200	8	50 mm U strip wrapping at 75 mm c/c		
		B11	1600	200	8	Fully FRP U wrap		
4	CFRP depth	B12	1600	200	8	50 mm U strip wrapping at 225 mm c/c	1600	100
		B13	1600	200	8	50 mm U strip wrapping at 175 mm c/c		
		B14	1600	200	8	50 mm U strip wrapping at 125 mm c/c		
		B15	1600	200	8	50 mm U strip wrapping at 75 mm c/c		
		B16	1600	200	8	Fully FRP U wrap		
5		B17	1600	200	8	50 mm U strip wrapping at 225 mm c/c	1600	150
		B18	1600	200	8	50 mm U strip wrapping at 175 mm c/c		
		B19	1600	200	8	50 mm U strip wrapping at 125 mm c/c		
		B20	1600	200	8	50 mm U strip wrapping at 75 mm c/c		
		B21	1600	200	8	Fully FRP U wrap		
6		B22	1600	200	8	50 mm U strip wrapping at 225 mm c/c	1600	200
		B23	1600	200	8	50 mm U strip wrapping at 175 mm c/c		
		B24	1600	200	8	50 mm U strip wrapping at 125 mm c/c		
		B25	1600	200	8	50 mm U strip wrapping at 75 mm c/c		
		B26	1600	200	8	Fully FRP U wrap		

2.4. Validation Process

The model validation is conducted in this study for the experimental study performed by Gesund et al. [25]. Bending and twisting moments at failure as well as the strain in the center bar of longitudinal reinforcement are compared with the NLFEA results. Figure 7 and Table 3 show good agreements between the finite element method and experimental results.

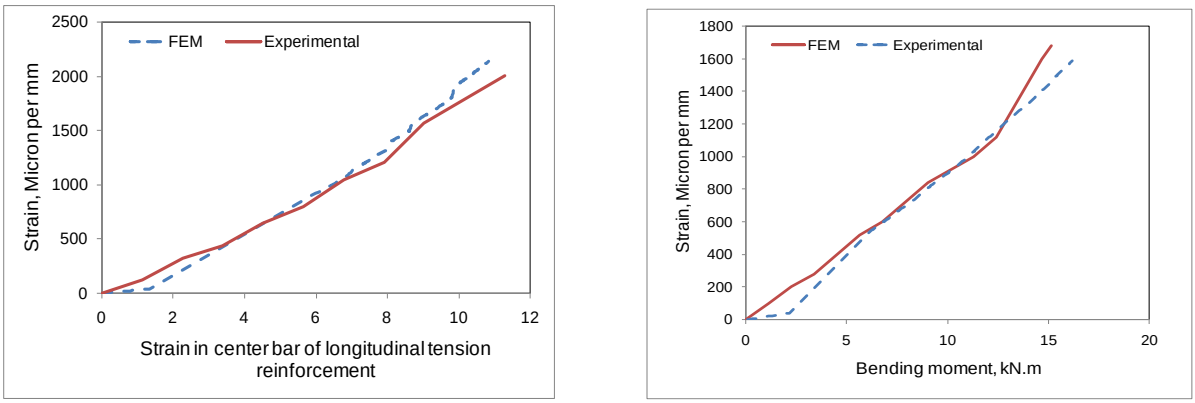

(a) Beam 2 **(b) Beam 4**

Figure 7. Validation of the NLFEA results.

Table 3. Validation summary.

Beam number	Torsion to Bending moment ratio	Bending moment at failure (kN.m)		The torsional moment at failure (kN.m)		Absolute Error %
		Experiment	FEM	Experiment	FEM	
2	1	11.52	10.9	11.52	10.9	5.3
4	0.5	15.14	16.2	7.6	8.1	–6.9

3. Results and Discussion

3.1. Load-Deflection and Torsion-Twist Behavior

Both the torsion-twist and load-deflection curves consist of three regions; the first region represents the stiffness for the un-cracked beam. The second region for the cracked beam. Whiles, the third region relates to the damaged cross-section with large cracks, yielding of steel and CFRP failure. Table 4 illustrates the obtained results for all simulated models. The slope of each region of the load-deflection curves gives the flexural stiffness of the corresponding beam. All strengthened beams represent higher stiffness compared to the control beam in the three regions. Table 4 also shows the calculated stiffness in each region for all simulated models.

Table 4. Results for all simulated models.

Group number	Model number	Ultimate load (kN)	Ultimate deflection(mm)	Ultimate torsion (kN.m)	Ultimate angle of twist (rad)	Stiffness (kN/mm)		
						Region 1	Region 2	Region 3
Control beams	BC1	22.28	3.05	06.68	0.0120	21.50	1.46	5.02
	BC2	24.26	2.36	7.27	0.0117	31.60	1.81	8.68
	BC3	26.77	1.73	8.03	0.0110	34.70	3.63	13.3
1	B1	44.10	4.88	13.22	0.0320	23.50	2.82	8.54
	B2	45.30	3.58	13.80	0.0237	34.60	3.18	11.8
	B3	49.20	2.69	14.75	0.0220	54.00	5.54	16.7
2	B4orB1	44.10	4.88	13.22	0.0320	23.50	2.82	8.54
	B5	36.20	4.14	10.87	0.0260	23.30	2.54	8.00
	B6	32.80	4.00	9.86	0.0230	23.10	2.40	7.82
3	B7	24.82	3.39	07.44	0.0142	21.60	1.48	5.58
	B8	25.63	3.44	07.68	0.0143	21.70	1.54	5.73
	B9	26.24	3.52	07.87	0.0152	22.30	1.69	5.78
	B10	27.36	3.60	08.21	0.0155	22.50	1.79	6.00
	B11	36.21	3.94	10.86	0.0248	23.10	2.38	7.91
4	B12	25.86	3.57	07.75	0.0152	21.70	1.52	5.74
	B13	26.45	3.61	07.93	0.0155	22.20	1.57	5.78
	B14	27.38	3.68	08.21	0.0160	22.60	1.73	5.83
	B15	29.03	3.84	08.71	0.0174	22.70	1.91	6.04
	B16	38.84	4.25	11.65	0.0252	23.20	2.49	8.00
5	B17	28.25	3.97	08.47	0.0183	22.20	1.57	5.87
	B18	29.51	4.08	08.85	0.0192	22.40	1.60	5.91
	B19	30.10	4.13	09.02	0.0193	22.70	1.78	6.00
	B20	31.52	4.21	09.45	0.0196	22.90	1.96	6.07
	B21	42.60	4.61	12.81	0.0266	23.30	2.76	8.46
6	B22	31.57	4.43	09.34	0.0225	22.40	1.59	5.91
	B23	32.43	4.45	09.65	0.0231	22.60	1.62	6.12
	B24	34.60	4.56	10.01	0.0237	22.90	1.76	6.15
	B25	36.20	4.81	10.86	0.0242	23.10	1.97	6.18
	B26orB1	44.1	4.88	13.22	0.0320	23.50	2.82	8.54

3.2. Ductility and Strength ratios

The ductility indicates how much the strengthened RC beams can sustain deformations without failure. The ductility ratio is defined as the ratio of the ultimate deflection of the strengthened beam to the ultimate deflection of the control beam. Similarly, strength ratio also predicts the increase of load that the model can sustain. Table 5 shows the ductility and strength ratios for all simulated models.

3.3. CFRP strain

Figure 8 shows the typical distribution of CFRP strain through its depth for the first group. It is noticed that all simulated beams had CFRP strain below the maximum value of 0.015 as mentioned in Table 2.

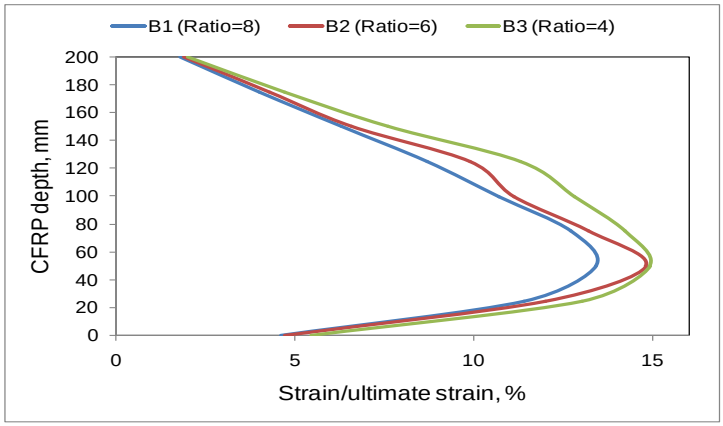

Figure 8. Typical CFRP strain for Group 1 versus ultimate strain.

Table 5. Enhancement percentage to control beam for all investigated parameters.

Group number	Model number	Torsional strength ratio	Flexural ductility ratio	Torsional ductility ratio	Percent enhancement in Stiffness			The percentage of CFRP strain to the ultimate strain
					Region 1	Region 2	Region 3	
Control beams	BC1	---	---	---	---	---	---	---
1	B1	83	55	100	109	193	170	13.4
	B2	98	60	167	115	175	135	14.8
	B3	62	36	117	155	152	125	15.0
2	B4 or B1	47	31	92	109	193	170	15.0
	B5	11	11	18	108	174	159	8.0
	B6	15	13	19	107	164	155	6.2
3	B7	18	15	27	100	101	111	1.5
	B8	23	18	29	101	105	114	2.0
	B9	71	29	107	104	115	115	2.0
	B10	16	17	27	105	122	119	2.7
	B11	19	18	29	107	163	158	8.0
4	B12	23	21	33	101	104	114	3.4
	B13	30	26	45	103	107	115	3.5
	B14	74	39	110	105	118	116	3.7
	B15	27	30	53	106	130	120	5.0
	B16	32	34	60	108	170	159	10.4
5	B17	35	35	61	103	108	117	4.9
	B18	41	38	63	104	110	118	5.1
	B19	91	51	122	106	122	119	6.0
	B20	42	45	88	107	134	121	6.0
	B21	46	46	93	108	189	169	13.7
6	B22	55	50	98	104	109	118	5.0
	B23	62	58	102	105	111	122	6.2
	B24	98	60	167	107	123	123	7.0
	B25	98	75	160	107	135	123	7.0
	B26 or B1	87	56	103	109	193	170	15.0

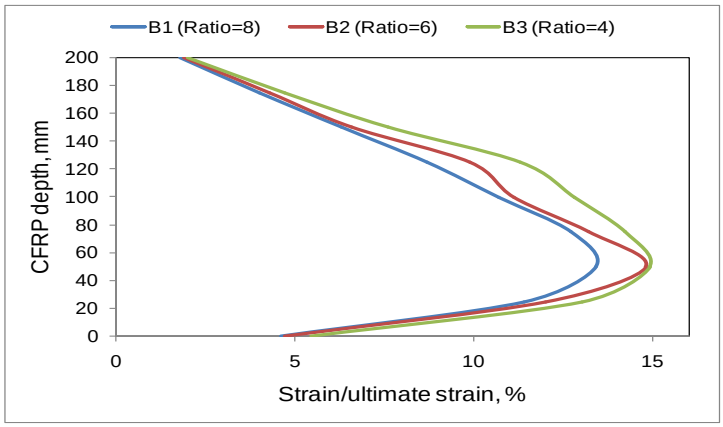

Figure 8. Typical CFRP strain for Group 1 versus ultimate strain.

3.4. Failure Mode

Figure 9 shows the crack pattern for the typically simulated beams. The first crack at an integration point is shown with a red circle outline, the second crack with a green outline, and the third crack with a blue outline. The first crack initiated from the support and then propagated towered the top of the beam in a diagonal shape. Due to the lack of CFRP wrapping along the control beam, this propagation spreads at a faster rate with individual cracks along the beam compared to the strengthened beams.

The FRP helps in distribution the stresses on the whole body of the beam. Also, the cracks were smaller and closer to each other, giving higher strength and capacity for those beams. All strengthened beams show almost similar diagonal cracks initiation. This due to the reality of similar loading and boundary conditions and the reinforcement details. However, the fully FRP U- wrap inhibits the propagation of crakes more than FRP strips. The beam strengthened with Fully FRP U wrap could sustain higher loads and deflections. The failure occurred due to the substantial wide diagonal cracks and concrete crushing followed by FRP failure.

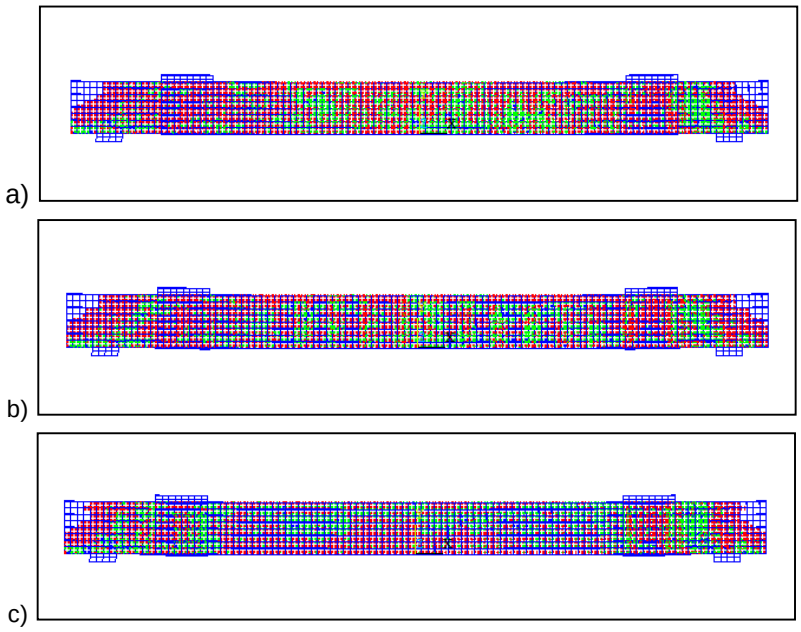

Figure 9. Crack pattern at failure: (a) control beam, (b) strengthened beams using FRP strips, and (c) strengthened beam using fully FRP U-wrap.

3.5. Effect of the clear span to depth ratio

To study the influence of the clear span to depth ratio factor, group 1 consists of three beams. B1, B2, and B3 are modeled with 8, 6 and 4 ratios, respectively. All of them are strengthened using fully CFRP U wrap. The torsional strength of the strengthened beams in this group is improved by 198 %, 187 % and 183 % for B1, B2, and B3, respectively. The flexural ductility is improved by 175 %, 156 % and 155 % over the control beam for B1, B2, and B3, respectively. While the torsional ductility is enhanced by 260 %, 203 % and 200 % for B1, B2, and B3, respectively, as shown in Table 5. Figure 10(a) and Figure 10(b) show the load-deflection and torsion-twist curves for group 1. It is noticed that the increase in the ratio leads to more increase in the flexural and torsional ductility. While the ultimate load that the beam can sustain decreases. Figure 10(c) shows the comparison between the three ratios to the ultimate load, ultimate deflection, and the ultimate angle of twist.

Furthermore, the results show the enhancement in the FRP strain and the stiffness at the three regions of the load-deflection curve. The percentage of CFRP strain value to the ultimate strain is 13.4 %, 14.8 %, and 15 % for B1, B2, and B3, respectively (Table 5). The stiffness at the initial part of the load-deflection curve is enhanced by 109 %, 115 %, and 155 % for B1, B2, and B3, respectively. In the second part the stiffness increases by 193 %, 175 % and 152 % for B1, B2, and B3, respectively. In the third part the stiffness increases by 170 %, 135 % and 125 % for B1, B2, and B3, respectively, as shown in Table 5.

3.6. Effect of CFRP length

To investigate the effect of CFRP length, a parametric study in group 2 is conducted for three different lengths; 1600 mm, 1100 mm and 800 mm. The torsional strength of the beams is enhanced by 198 %, 162 %, and 147 % for B4, B5, and B6, respectively. The flexural ductility is enhanced by 160 %, 136 % and 131 % for B4, B5, and B6, respectively, while the torsional ductility is enhanced by 267 %, 217 % and 192 % for B4, B5, and B6, respectively (Table 5). The ultimate load, ultimate torsion, and the ductility of the RC beam increase as the length of the CFRP increases. Figure 11 also verifies this conclusion.

The load-deflection and torsion-twist curves are shown in Figure 11(a) and Figure 11(b), respectively. The percentage of CFRP strain value to the ultimate strain is 15 %, 8 %, and 6.2 % for B4, B5, and B6, respectively. The stiffness at the initial part is enhanced by 109 %, 108 %, and 107 % for B4, B5, and B6, respectively. In the second part the stiffness increases by 193 %, 174 % and 164 % for B4, B5, and B6, respectively. In the third part the stiffness increases by 170 %, 159 % and 155 %for B4, B5, and B6, respectively (Table 5). These results indicate that increasing the length of CFRP lead to more enhancements in the FRP strain. Also, the stiffness at the three regions of the load-deflection curve.

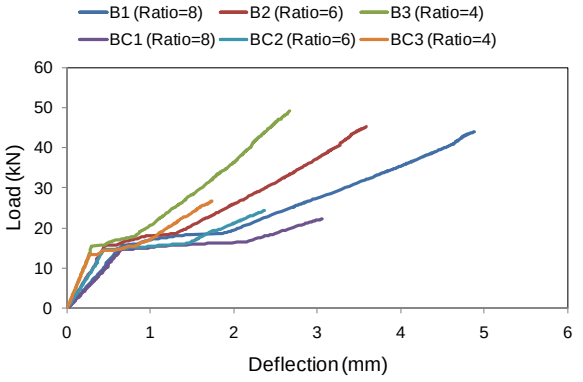

(a) Load-deflection curve

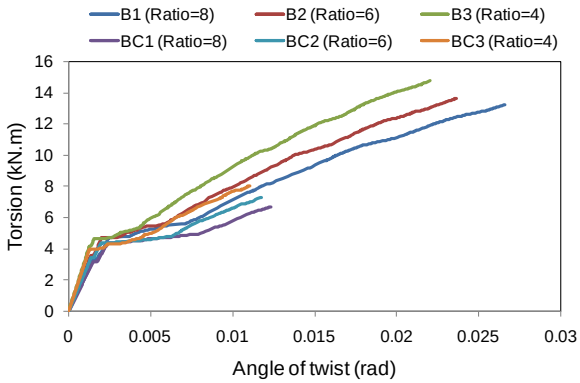

(b) Torsion-angle of twist curve

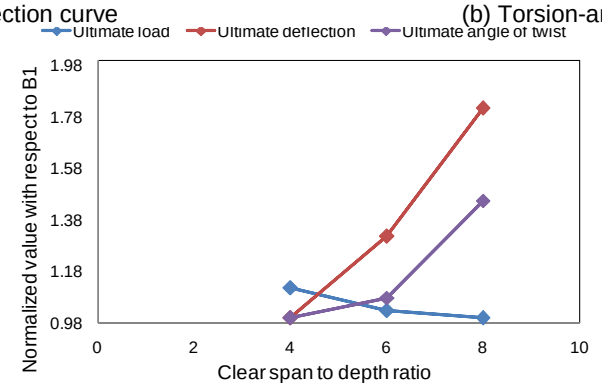

(c) Comparison with respect to the ultimate load, ultimate deflection and ultimate angle of twist

Figure 10. Group 1 results

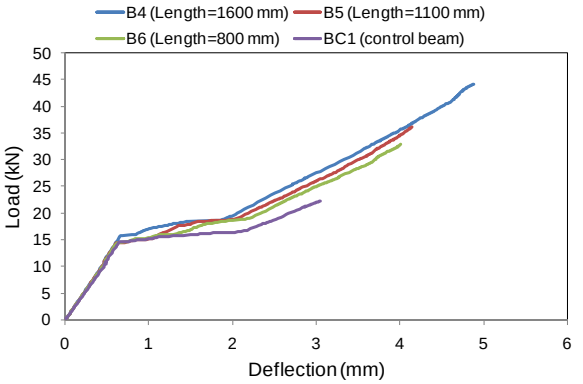

(a) Load-deflection curve

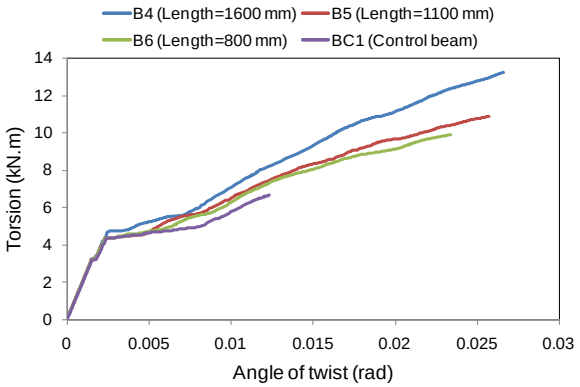

(b) Torsion-angle of twist curve

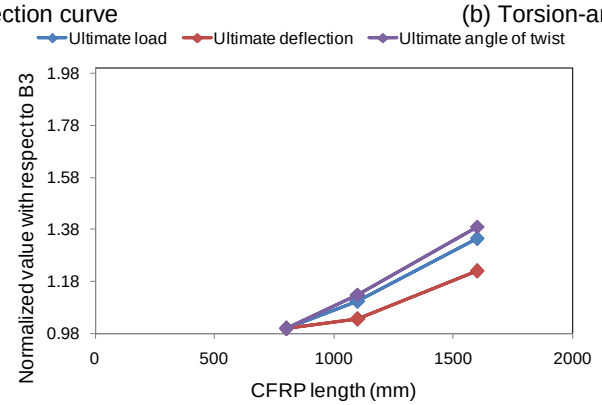

(c) Comparison with respect to the ultimate load, ultimate deflection and ultimate angle of twist

Figure 11. Group 2 results.

3.7. Effect of the CFRP Depth and CFRP Strip Spacing

To study the effect of the CFRP depth parameter, this study conducts four different depth of the beam; 50 mm, 100 mm, 150 mm, and 200 mm for groups 3, 4, 5, and 6, respectively. Each depth group includes five beams with different CFRP configuration of U strip wrapping with the spacing of 75 mm,125 mm,175 mm and 225 mm. The fifth beam is considered with fully U-wrap. Group 3 exhibits strength enhancement by 111 %, 115 %, 118 %, 123 % and 171 % for B7, B8, B9, B10, and B11, respectively (Figure 12 and Table 5). The flexural ductility is enhancement by 111 %, 113 %, 115 %, 118 % and 129 % for B7, B8, B9, B10, and B11, respectively. While the torsional ductility is enhanced by 118 %, 119 %, 127 %, 129 % and 207 % for B7, B8, B9, B10, and B11, respectively (Figure 12 and Table 5). The percentage of CFRP strain value to the ultimate strain is 1.5 %, 2 %, 2 %, 2.7 and 8 % for B7, B8, B9, B10, and B11, respectively (Figure 12 and Table 5). The stiffness at the initial region of the load-deflection curve is enhanced by 100.4 %, 101 %, 103.7 %, 104.7 %, and 107.4 % for B7, B8, B9, B10, and B11, respectively (Table 5). In the second region the stiffness increases by 101 %, 105 %, 115 %, 122 % and 163 % for B7, B8, B9, B10, and B11, respectively (Table 5). In the third region the stiffness increases by 111 %, 114 %, 115 %, 119 % and 158 % for B7, B8, B9, B10, and B11, respectively (Figure 12 and Table 5).

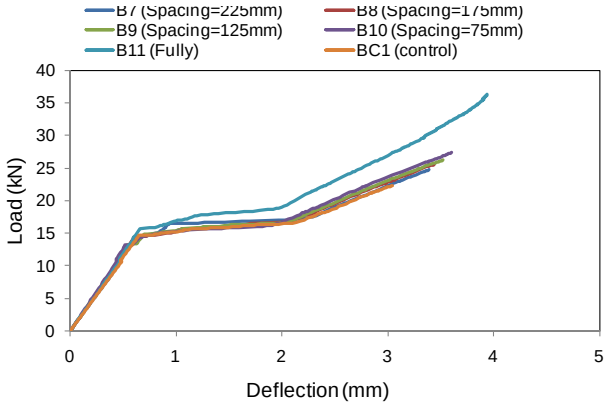

(a) Load-deflection curve

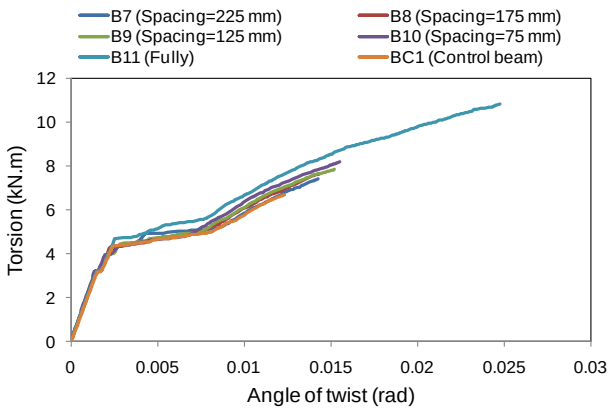

(b) Torsion-angle of twist curve

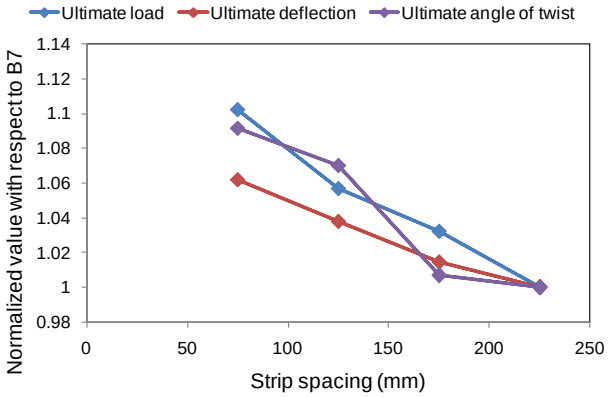

(c) Comparison with respect to the ultimate load, ultimate deflection and ultimate angle of twist

Figure 12. Group 3 results

Group 4 shows strength enhancement by 116 %, 119 %, 123 %, 130 % and 174 % for B12, B13, B14, B15, and B16, respectively (Table 5). The flexural ductility is enhanced by 117 %, 118 %, 121 %, 126 % and 139 % for B12, B13, B14, B15, and B16, respectively. While the torsional ductility is enhanced by 127 %, 129 %, 133 %, 145 % and 210 % for B12, B13, B14, B15, and B16, respectively (Figure 13 and Table 5). The percentage of CFRP strain value with respect to the ultimate strain is 3.4 %, 3.5 %, 3.7 %, 5 % and 10.4 % for B12, B13, B14, B15 and B16, respectively (Figure 13 and Table 5). The stiffness at the initial region of load-deflection curve is enhanced by 101 %, 103 %, 105 %, 106 %, and 108 % for B12, B13, B14, B15, and B16 respectively (Table 5). In the second region the stiffness increases by 104 %, 107 %, 118 %, 130 % and 170 % for B12, B13, B14, B15, and B16, respectively. In the third region the stiffness increases by 114 %, 115 %, 116 %, 120 % and 159 % for B12, B13, B14, B15, and B16, respectively (Figure 13 and Table 5).

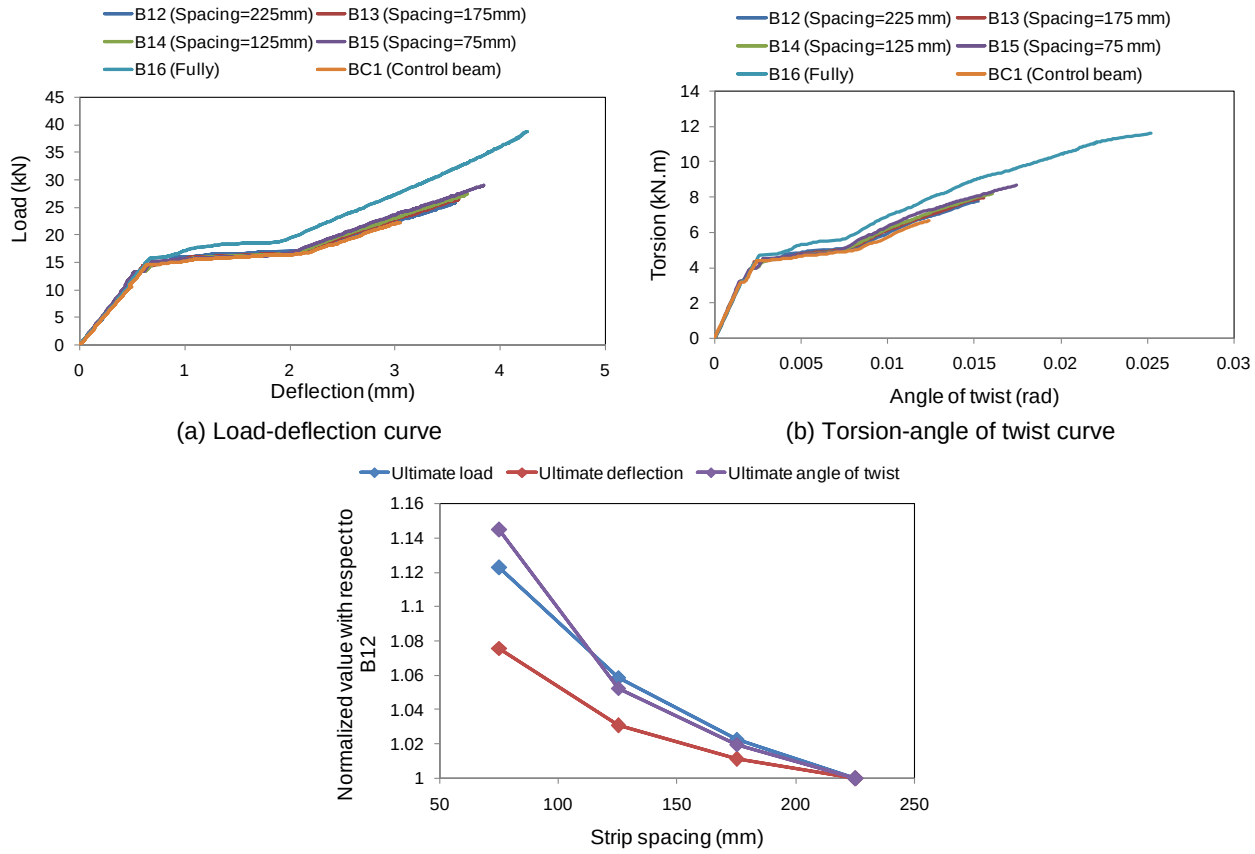

(a) Load-deflection curve

(b) Torsion-angle of twist curve

(c) Comparison with respect to the ultimate load, ultimate deflection and ultimate angle of twist

Figure 13. Group 4 results.

Group 5 exhibits torsional strength enhancement by 127 %, 132 %, 135 %, 141 % and 191 % for B17, B18, B19, B20, and B21, respectively (Table 5). The flexural ductility is enhanced by 127 %, 132 %, 135 %, 141 % and 191 % for B17, B18, B19, B20, and B21, respectively. While the torsional ductility is enhanced by 188 %, 193 %, 198 %, 202 % and 267 % for B17, B18, B19, B20, and B21, respectively (Figure 14 and Table 5). The percentage of CFRP strain value to the ultimate strain is 4.9 %, 5.1 %, 6 %, 6 % and 13.7 % for B17, B18, B19, B20, and B21, respectively (Figure 14 and Table 5). The stiffness at the initial region of the load-deflection curve is enhanced by 103 %, 104 %, 106 %, 107 %, and 108.4 % for B17, B18, B19, B20, and B21, respectively. In the second region the stiffness increases by 108 %, 110 %, 122 %, 134 % and 189 % for B17, B18, B19, B20 and B21, respectively. In the third region, the stiffness increases by 117 %, 118 %, 119 %, 121 % and 169 % for B17, B18, B19, B20, and B21, respectively (Figure 14).

Group 6 exhibits torsional strength enhancement by 142 %, 146 %, 155 %, 162 % and 218 % for B22, B23, B24, B25 and B26, respectively (Figure 15 and Table 5). The flexural ductility is enhanced by 145 %, 146 %, 150 %, 158 % and 160 % for B22, B23, B24, B25 and B26, respectively (Figure 15). The percentage of CFRP strain value to the ultimate strain is 5 %, 6.2 %, 7 %, 7 % and 15 % for B22, B23, B24, B25, and B26, respectively (Figure 15 and Table 5). The stiffness at the initial region of the load-deflection curve is enhanced by 104 %, 105 %, 107 %, 107.4 %, and 109 % for B22, B23, B24, B25, and B26, respectively (Figure 15 and Table 5). At the second region the stiffness increases by 109 %, 111 %, 123 %, 135 % and 193 % for B22, B23, B24, B25 and B26, respectively (Figure 15 and Table 5). At the third region the stiffness increases by 118 %, 122 %, 122.5 %, 123 % and 170 % for B22, B23, B24, B25 and B26, respectively (Figure 15 and Table 5). Figure 10 to Figure 15 shows the load-deflection curves, torsion-twist curves, and the comparison between the models of each group that are 3, 4, 5, and 6. It is clear that decreasing strip spacing. The beam can sustain higher load, deflection, torsion and hence higher angle of twist.

For the same CFRP strip spacing with different depth, the enhancement increases as the CFRP depth increases, as shown in Figure 16 and Table 5. The model wrapped using fully FRP U-wrap records the highest values with the enhancement range of (171–198 %) for ultimate torsional strength and (207–267) % for ultimate torsional ductility. Furthermore, the results show better enhancement in the FRP strain and the stiffness at the three regions of the load-deflection curve as increasing the depth of CFRP and decreasing the strip spacing.

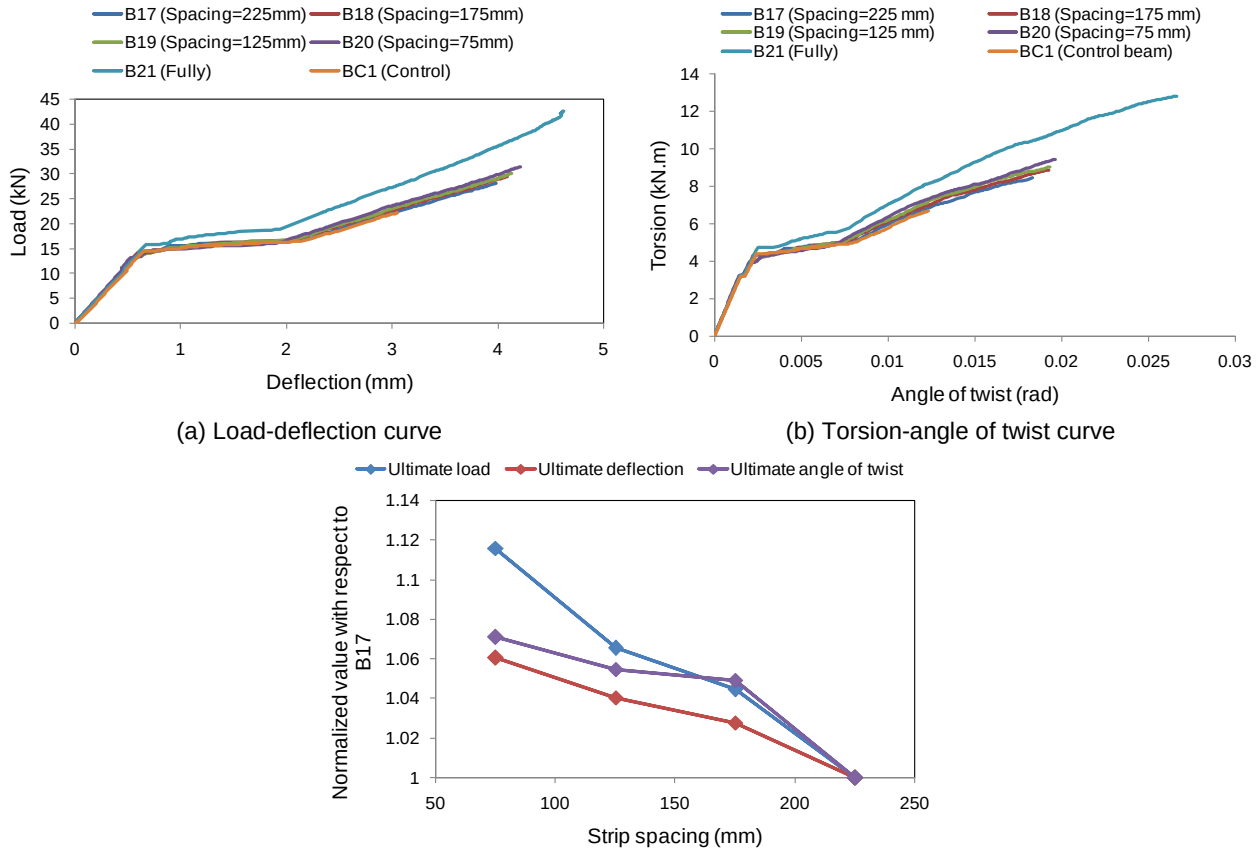

(a) Load-deflection curve

(b) Torsion-angle of twist curve

(c) Comparison with respect to the ultimate load, ultimate deflection and ultimate angle of twist

Figure 14. Group 5 results.

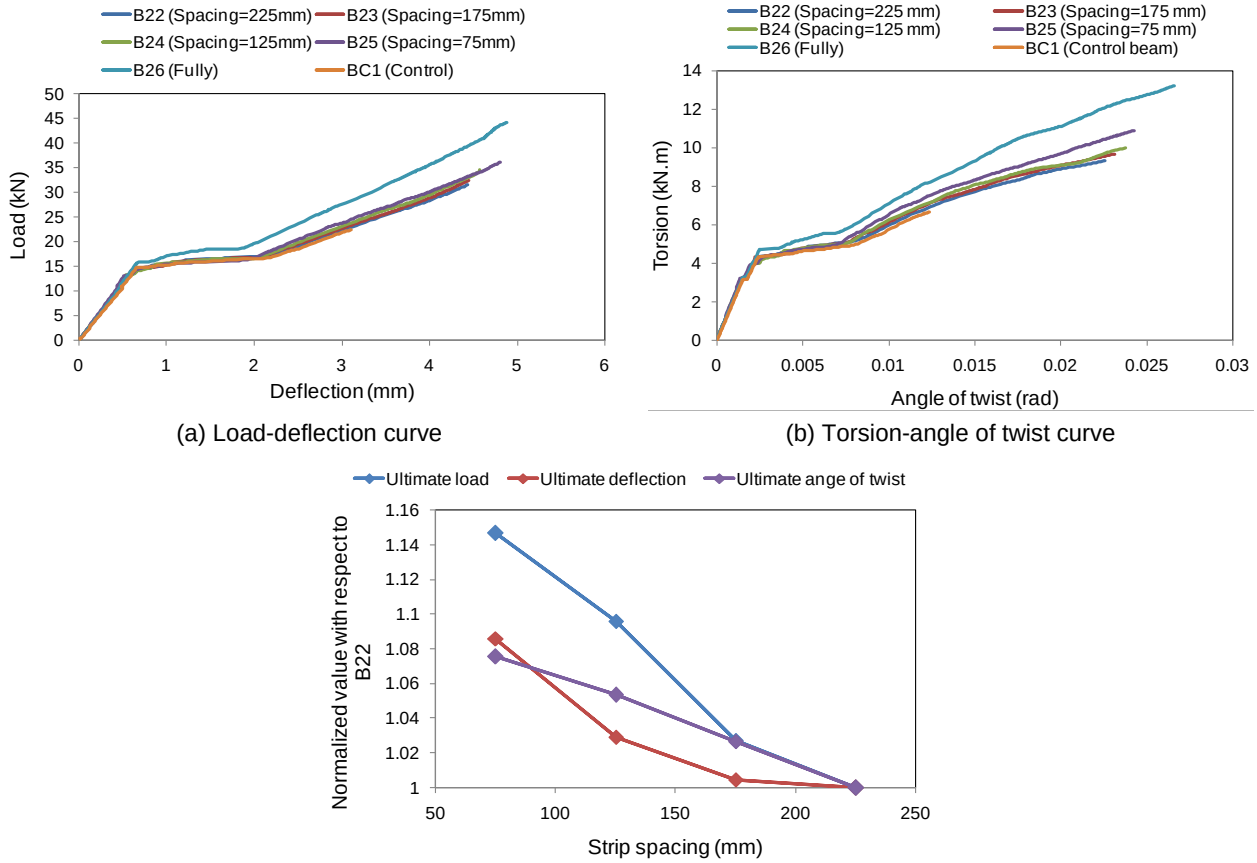

(a) Load-deflection curve

(b) Torsion-angle of twist curve

(c) Comparison with respect to the ultimate load, ultimate deflection and ultimate angle of twist

Figure 15. Group 6 results.

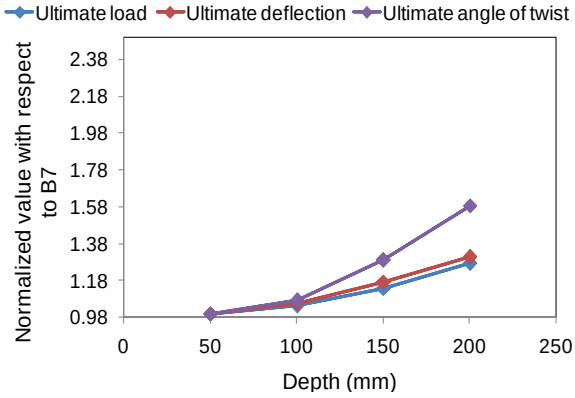

(a) B7, B12, B17 and B22 of 225 mm strip spacing

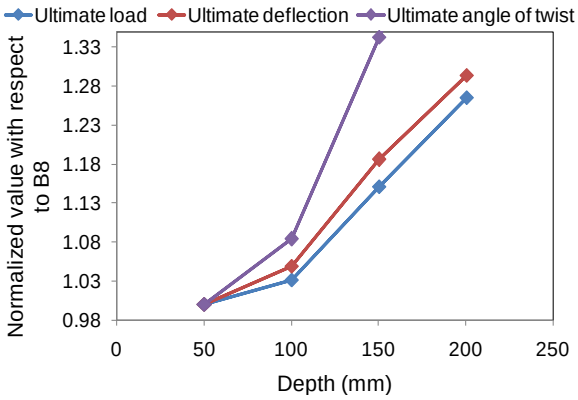

(b) B8, B13, B18 and B23 of 175 mm strip spacing

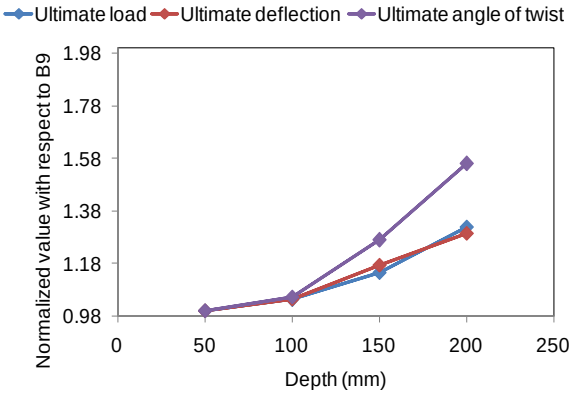

(c) B9, B14, B19 and B24 of 125 mm strip spacing

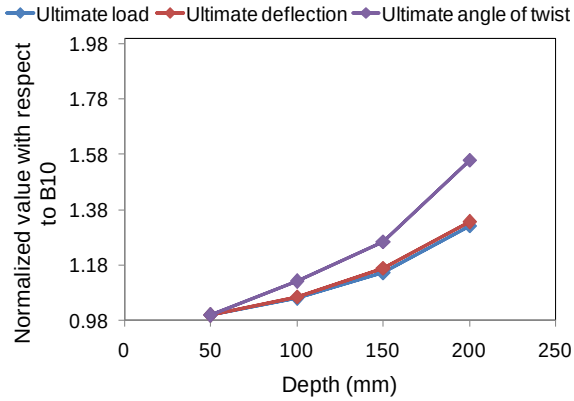

(d) B10, B15, B20 and B25 of 75 mm strip spacing

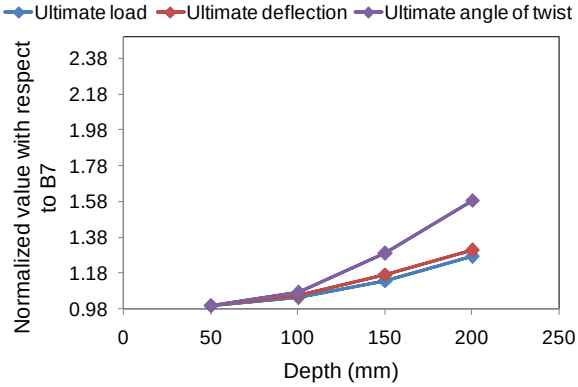

(e) B11, B16, B21 and B26 of fully U wrap

Figure 16. Comparison between strip spacing to the ultimate load, ultimate deflection and ultimate angle of twist,

3.8. Comparison of NLFEA with other results

Comparison of NLFEA with Vishnu et al. [1], the bending moment and torque for all specimens at first crack are closed to NLFEA. Due to FRP torsional resistance of beam is increased in all types of wrapping configuration. Maximum bending moment and torsional moment are resisted by Full Transverse FRP wrapping. Also, all specimens wrapped with GFRP show better torsional resistance compared to the control specimen. Results show an increase in structural behavior of the strengthened beam is almost the same performance as the NLFEA. Besides, Vishnu et al. [1] reached the same conclusion as NLFEA that the fully U wrap strengthening technique of RC beam with FRP is more efficient in resisting torsional moment compared to the vertical strip.

4. Conclusions

1. The three-dimensional finite element model provided by this study was suitable to predict the behavior of strengthened RC beams subjected to combined bending and torsion. The mode of failure, ultimate strength, ductility, stiffness, and FRP strain can be accurately predicted.

2. As increasing the length of CFRP, the beam can sustain higher load, deflection, moment and hence higher orientation.

3. The efficiency of using CFRP strips increases as decreasing the center to center spacing between them. For the same spacing, this efficiency increases as increasing the depth of CFRP.

4. Using fully FRP U wrap is more effective than CFRP strips with higher torsional strength and ductility.

5. All strengthened beams represent higher stiffness compared to the control beam in the three regions of the load-deflection curves.

6. The control beam shows a faster rate of diagonal crack propagation than the strengthened beams. This is due to the lack of CFRP wrapping along the beam. The failure occurred after substantial wide diagonal cracks and concrete crushing followed by CFRP rupture.

References

1. Kongjian, Shen, Shui Wan, Y.L. Mo, Zhengwen, Jiang. Theoretical analysis on full torsional behavior of RC beams strengthened with FRP materials. Composite Structures. 2018. 183(1). Pp. 347–357. DOI: 10.1016/j.compstruct.2017.03.084.
2. Jariwala, V.H., Patel, P, Purohit, S.P. Strengthening of RC beams subjected to combined torsion and bending with GFRP composites. Procedia Engineering. 2013. 51(1). Pp. 282–289. DOI: 10.1016/j.proeng.2013.01.038
3. Amulu, C.P., Zeagu, C.A. Experimental and analytical comparison of torsion, bending moment and shear forces in reinforced concrete beams using BS 8110, euro code 2 and ACI 318 provisions. Nigerian Journal of Technology. 2017. 36(3). Pp. 705–711. DOI:10.4314/njt.v36i3.7.
4. Meyyada, Y. Alabdulhady, Lesley, H. Sneed, Christian, Carloni. Torsional behavior of RC beams strengthened with PBO-FRCM composite–An experimental study. Engineering Structures. 2017. 136(1). Pp. 393–405. DOI: 10.1016/j.engstruct.2017.01.044
5. Gonzalez-Libreros, J.H., Sneed, L.H., D'Antino, T., Pellegrino, C. Behavior of RC beams strengthened in shear with FRP and FRCM composites. Engineering Structures. 2017. 150(1). Pp. 830–842. DOI: 10.1016/j.engstruct.2017.07.084
6. Shraddha, B. Tibhe, Vijaykumar, R. Rathi. Comparative Experimental Study on Torsional Behavior of RC Beam Using CFRP and GFRP Fabric Wrapping. Procedia Technology. 2016. 24(1). Pp. 2212–0173. DOI: 10.1016/j.protcy.2016.05.020
7. Rahal, K.N., Collins, M.P. Combined torsion and bending in reinforced and prestressed concrete beams. ACI Structural Journal. 2003. 100(2). Pp. 157–165. DOI: 10.14359/12479
8. Hii, AKY, Al-mahaidi, R., Asce, M. Torsional capacity of CFRP strengthened reinforced concrete beams. Journal of Composites for Construction. 2007. 11(1). Pp. 71–80. DOI:10.1061/(ASCE)1090-0268(2007)11:1(71).
9. Ghaidak Al-Bayati, Riadh Al-Mahaidi, M. Javad Hashemi, Robin Kalfat. Torsional strengthening of RC beams using NSM CFRP rope and innovative adhesives. Composite Structures. 2018. 187(1). Pp. 190–202. DOI: 10.1016/j.compstruct.2017.12.016
10. Ameli, M., Ronagh, H.R. Analytical method for evaluating ultimate torque of FRP strengthened reinforced concrete beams. Journal of Composites for Construction. 2007. 11(4). Pp. 384–390. DOI: 10.1061/(ASCE)1090-0268(2007)11:4(384).
11. Aravind, N., Samanta, A.K., Roy, D.S., Thanikal, J.V. Retrofitting of reinforced concrete beams using fiber reinforced polymer (FRP) composites–a review. Journal of Urban and Environmental Engineering. 2013. 7(1). Pp. 164–175. DOI: 10.4090/juee.2013.v7n1.164175.
12. Meyyada Y. Alabdulhady, Lesley H. Sneed, Omar I. Abdelkarim, Mohamed A. ElGawady. Finite element study on the behavior of RC beams strengthened with PBO-FRCM composite under torsion. Composite Structures. 2017. 179(1). Pp. 326–339. DOI: 10.1016/j.compstruct.2017.07.079
13. Al-Bayati, G., Kalfat, R., Al-Mahaidi, R., Hashemi, J. Experimental study on crack propagation of CFRP-strengthened RC beams subjected to torsion. Australian Journal of Structural Engineering. 2018. 19(4). Pp. 279–297. DOI: 10.1080/13287982.1523293.
14. Al-Bayati, G., Al-Mahaidi, R., Kalfat, R. Experimental investigation into the use of NSM FRP to increase the torsional resistance of RC beams using epoxy resins and cement-based adhesives. Construction and Building Materials. 2016. 124(1). Pp. 1153–1164. DOI: 10.1016/j.conbuildmat.2016.08.095.
15. Al-Bayati, G., Al-Mahaidi, R., Kalfat, R.. Torsional strengthening of reinforced concrete beams using different configurations of NSM FRP with epoxy resins and cement-based adhesives. Composite Structures. 2017. 168(1). Pp. 569–581. DOI: 10.1016/j.compstruct.2016.12.045
16. Deifalla, A., Ghobarah, A. Strengthening RC T-beams subjected to combined torsion and shear using FRP fabrics: Experimental study. Journal of composites for construction. 2010. 14(3). Pp. 301–311. DOI: 10.1061/(ASCE)CC.1943-5614.0000091.
17. Vishnu, H. Jariwala, Paresh, V. Patel, Sharadkumar, P. Purohit. Strengthening of RC Beams Subjected to Combined Torsion and Bending with GFRP Composites. Procedia Engineering. 2013. 51(1). Pp. 282–289. DOI: 10.1016/j.proeng.2013.01.038
18. Ghobarah, A., Ghorbel, M.N., Chidiac, S.E. Upgrading torsional resistance of reinforced concrete beams using fiber-reinforced polymer. Journal of Composites for Construction. 2002. 6(4). Pp. 257–263. DOI: 10.1061/(ASCE)1090-0268(2002)6:4(257).
19. Deifalla, A., Ghobarah, A. Full torsional behavior of RC beams wrapped with FRP: analytical model. Journal of Composites for Construction. 2010. 14(3). Pp. 289–300. DOI: 10.1061/(ASCE)CC.1943-5614.0000085
20. Mahmood, M.N. Nonlinear analysis of reinforced concrete beams under pure torsion. Journal of Applied Sciences. 2007. 7(22). Pp. 3524–3529. DOI: 10.3923/jas.2007.3524.3529
21. Prabaghar, A., Kumaran, G. Theoretical study on the behavior of rectangular concrete beams reinforced internally with GFRP reinforcements under pure torsion. International Journal of Civil and Structural Engineering. 2011. 2(2). Pp. 570–594. DOI: 10.6088/ijcser.00202010134.
22. Elwan, S.K. Torsion strengthening of RC beams using CFRP (parametric study). Journal of Civil Engineering. 2017. 21(4). Pp. 1273–1281. DOI: 10.1007/s12205-016-0156-7.
23. Zojaji, A.R. znd Kabir, M.Z. Analytical approach for predicting full torsional behavior of reinforced concrete beams strengthened with FRP materials. Scientia Iranica. 2012. 19(2). Pp. 51–63. DOI: 10.1016/j.scient.2011.12.004.
24. Ameli, M., Ronagh, H.R., Dux, P.F. Behavior of FRP strengthened reinforced concrete beams under torsion. Journal of Composites for Construction. 2007. 11(2). Pp. 192–200. DOI: 10.1061/(ASCE)1090-0268(2007)11:2(192)
25. Gesund, H., Schuette, F.J., Buchanan, G.R., Gray, G.A. Ultimate strength in combined bending and torsion of concrete beams containing both longitudinal and transverse reinforcement. Journal of the American Concrete Institute. 1964. 61(12). Pp. 1509–1522. DOI: 10.1680/macr.1968.20.64.155.

Contacts:

Rajai Al-Rousan, +962799887574; rzalrousan@just.edu.jo
Isra'a Abo-Msamh, +96227201000; iabomsamh@gmail.com